Viscosity of methane to 6 GPa and 673 K

Evan H. Abramson

Phys. Rev. E **84**, 062201 — Published 30 December 2011

DOI: 10.1103/PhysRevE.84.062201

Viscosity of methane to 6 GPa and 673K

EVAN H. ABRAMSON*

Department of Earth and Space Sciences, University of Washington, Seattle, USA

Receipt date: October 6, 2011

A rolling-sphere technique has been used to measure shear viscosities of (supercritical) fluid methane in the diamond-anvil cell between the temperatures of 294K and 673K, up to a pressure of 6 GPa. A correlation between a reduced viscosity and reduced residual entropy is shown to give a good account of much of the extant data, both from this study and the literature.

1. INTRODUCTION

As part of a program to determine the shear viscosities of small molecules to high densities, I present here measurements taken on methane for temperatures between 294K and 673K and up to the melting pressures. Methane is a subject of both experimental and theoretical interest; a sizeable body of data already exists at low and intermediate pressures as summarized in [1]. Data have also been taken up to 1 GPa at 273K [2] and at 298K [3], and to 0.08 GPa and a maximum temperature of 523K [4]. Given its nature as a psuedo-spherical molecule, it was interesting to see whether methane would continue to behave akin to a hard-sphere or, at higher densities, exhibit a "locking" of rotational motion as surmised in references [2, 3].

2. EXPERIMENTAL

The technique has been described in several previous publications [5-7]. High pressures were generated with diamond-anvil cells of a modified Merrill-Basset design, using anvils with ~650 μm diameter culets and gaskets of hardened Inconel 718. Both ruby [8] and Sm-doped SrB_4O_7 [9] were used to measure pressure with a typical precision of 0.02 GPa. The cell was loaded by immersion in cryogenic, liquid methane condensed from the gas (nominal purity 99.995%). The cell was placed in an oven and temperature was measured to an accuracy of 1K with chromel-alumel thermocouples located in proximity to the diamonds.

In addition to the pressure marker, each of the loads contained a single platinum sphere of ~40μm diameter. The cell and its enclosing oven were located on a combined tilt-rotation stage which allowed the plane of the diamond culets to be inclined with respect to the horizontal, typically between 15 and 30°, and the cell then to be rotated about the normal to the plane until the sphere was toward the top. As the sphere rolled down the plane of the lower diamond its trajectory was recorded with a video camera (100 frames/s). Plots of the speed against the sine of the angle of inclination formed straight lines the slopes of which were inversely proportional to the viscosity of the surrounding fluid. For any sphere the constant of proportionality could be determined by filling the cell with a fluid of known viscosity, in these experiments either toluene at 1 bar [10] or water at 0.1 GPa [11].

3. RESULTS

Measurements were taken on approximate isotherms of 294, 373, 473, 573 and 673K; results (Table I) are plotted in Fig. 1. The viscosities, η, are well represented by the equation [6]:

$$\ln(\eta)=\ln\{\eta_{dilute}\rho_0/[(B\text{-}1)\rho+\rho_0]\}+B\rho/(\rho_0-\rho) \qquad (1)$$

where ρ is the density, η_{dilute} the viscosity of the dilute gas [1] at the given temperature, and B and ρ_0 are constants for each isotherm. A simultaneous fit to all the data (curves through data in Fig. 1) with B=6.71+1.969x10^{-2}T and ρ_0(g cm^{-3})=0.799 + 4.055x10^{-3}T provides a root-mean-square misfit of 1.8%. Throughout this paper derived thermodynamic quantities (density and entropy) are taken from [12] in which the equation of state is described by an expansion of the Helmholtz energy in terms of density and (inverse) temperature, and other quantities are obtained by the appropriate combination of derivatives. Taking into account random uncertainties of the individual measurements in methane (the fractional uncertainty of the slope, δ, for each least-squares fit of rolling speed is given in Table 1) and also in the calibration of the various spheres, the absolute error of the overall fit to Eq. 1 is believed to be better than 4% over the range of the data.

Figure 2 shows deviations from the fits for pressures below 1.5 GPa, where current data may be compared with previously obtained values. Equation 1 typically underestimates viscosities along lower temperature isotherms at lower pressures, with the maximum error occurring at about the critical density (for methane, roughly 0.03 GPa at 298K). The general form of the deviations in Fig. 2 is thus expected, the maximum being comparable to that for carbon dioxide [13] while somewhat larger than for argon [14] and significantly larger than for nitrogen [15], presumably reflecting the progression toward smaller attractive forces in the series.

The correlation between a reduced viscosity, η_{red}, and reduced residual entropy, s, noted [13-15] in other systems holds also for methane as shown in Fig. 3. The variables of the plot are:

$$\eta_{red}=\eta\rho_{melt}^{-2/3}(mkT)^{-1/2} \quad \text{and} \quad s=-(S-S_{ideal})/Nk \qquad (2)$$

where ρ_{melt} is the particle density of the fluid at its melting pressure (at the relevant temperature [16]), m is the particle mass, k Boltzmann's constant, and S is the entropy, while S_{ideal} is the entropy the fluid would have if it were an ideal gas at the same density and temperature. Note that in Rosenfeld's original proposal [17] viscosity was reduced by the fluid density at the relevant temperature *and* pressure; since this causes a divergence as density tends to zero I use here an altered definition in which a reasonable defining distance is taken to be proportional to the cube-root of the (liquid) molecular volume at the melting point, that is, the closest one may pack the molecules at any particular temperature before the solid becomes the stable phase. The figure contains current experimental results along with viscosities previously reported for the supercritical fluid between 0 and 1 GPa, and in the sub-critical liquid. The scale at the top indicates the ratio of the density to the critical density for the 298K isotherm. At the highest pressure in the study (and 684K) the density is a factor of 4.9 larger than the critical density.

The data of Fig. 3 may be approximated by a straight line in the semilogarithmic plot, $\ln(\eta_{red})$=0.860s-2.05 . Deviations from this fit are shown in Fig. 4. Uncertainty in entropy can account for some of the deviation, especially when extrapolating the equation of state to pressures in excess of 1 GPa, however the 1% uncertainty estimated [12] for specific heats, integrated between the triple point and 298K, leads to an error of only ~0.07 e.u. and is unlikely to be the source for the large departure of the sub-critical liquid as it approaches the triple point. The correlation does yield an excellent account of the higher temperature data and, insofar as the entropy is adequately known, is expected to be a better predictor of viscosities in extrapolation than Eq. 1. It seems likely therefore that the large deviations to lower viscosities of the 473K and 523K points of [4] is indicative of systematic error in those experiments; this view is corroborated by comparison of the 273K and 298K data of [4] with those of [2, 3]. Viscosities at higher pressures and temperatures may be predicted by calculating for each point a value of s, then using the line in Fig. 3 to define a value of η_{red} and thence η. In Fig. 1 a curve of predicted viscosities at 1000K is drawn in this manner.

Fragiadakis and Roland [18] have shown that fluids of small, nonassociating molecules have kinetic properties which, when suitably reduced, scale to the quantity T/ρ^{γ} with γ a constant of the system; further, for molecules approximating hard spheres γ is found to have a value equal to the thermodynamic quantity $\Gamma=d\ln(T_{melt})/d\ln(\rho_{melt})$. One of the systems considered was methane which at lower pressures was found to have viscosities and, separately, melting densities scaling as $\gamma\approx\Gamma\approx4$. Fig. 5 demonstrates that for reduced viscosities the utility of this scaling persists up to the pressures and temperatures of the current study. Again, viscosities along the line of vapor-liquid equilibrium are seen to depart from the higher temperature data; a somewhat tighter correlation of the latter can be achieved with $\gamma=3.9$, but only at the cost of increasing deviation along the vapor-liquid line. The interesting equation noted in [18] between γ and Γ does not hold at higher pressures and temperatures. Indeed, Γ is not constant over the larger range of this extended data set; as seen in the inset to Fig. 5, it decreases from a maximum of 4.4 at 120K down to a value of 2.8 for the 673K melt.

Van der Gulik et al. [2, 3] suggested that at the highest pressures of their experiments (0.8 GPa- 1.0 GPa) and close to the melting point the viscosities increased with pressure more rapidly than expected, possibly due to a locking of rotational motion. The current data, while not as precise as the former, do indicate a continuation of the trend noted in the 298K study. Still, at a comparable temperature (294K) the maximum density in this study is 6% higher than in the previous while the present 684K data extend to a value 39% higher. It seems likely that such a large increase in what was already a liquid-like packing of molecules would have caused a fluid on the verge of rotational locking to demonstrate a radical divergence in viscosity, even at the larger temperature.

ACKNOWLEDGEMENTS

This work was supported by the Department of Energy, Contract No. DE-FG52-09NA29466.

References

* email: evan@ess.washington.edu

[1] D. G. Friend, J. F. Ely and H. Ingham, J. Phys. Chem. Ref. Data **18**, 583 (1989).
[2] P. S. van der Gulik, R. Mostert and H. R. van den Berg, Fluid Phase Equilib. **79**, 301 (1992).
[3] P. S. van der Gulik, R. Mostert and H. R. van den Berg, Physica A (Amsterdam) **151**, 153 (1988).
[4] I. F. Golubev, *Viscosity of Gases and Gas Mixtures (A Handbook)* (Israel Program for Scientific Translations, Jerusalem, 1970), p.83.
[5] H. E. King, Jr., E. Herbolzheimer and R. L. Cook, J. Appl. Phys. **71**, 2071 (1992).
[6] E. H. Abramson, J. Chem. Phys. **122**, 84501 (2005).
[7] E. H. Abramson, Phys. Rev. E **76**, 051203 (2007).
[8] H. K. Mao, J. Xu and P. M. Bell, J. Geophys. Res. **91**, 4673 (1986).
[9] E. H. Abramson and J. M. Brown, Geochim. Cosmochim. Acta **68**, 1827 (2004).
[10] C. L. Yaws, *Handbook of Transport Property Data: Viscosity, Thermal Conductivity, and Diffusion Coefficients of Liquids and Gases* (Gulf Publishing Co., Houston, 1995), p.43.
[11] R. A. Perkins, A. Laesecke, D. G. Friend, J. V. Sengers, M. J. Assael, I. N. Metaxa, E. Vogel, R. Mares and K. Miyagawa, J. Phys. Chem. Ref. Data **38**, 101 (2009).

[12] U. Setzmann and W. Wagner, J. Phys. Chem. Ref. Data **20**, 1061 (1991).
[13] E. H. Abramson, Phys. Rev. E **80**, 021201 (2009).
[14] E. H. Abramson, High Pressure Res. **31**, 544 (2011).
[15] E. H. Abramson and H. West-Foyle, Phys. Rev. E **77**, 041202 (2008).
[16] E. H. Abramson, High Pressure Res. **31**, 549 (2011).
[17] Y. Rosenfeld, Phys. Rev. A **15**, 2545 (1977).
[18] D. Fragiadakis and C. M. Roland, Phys Rev. E **83**, 031504 (2011).

Figure Captions

FIG. 1. Measured viscosities are plotted against pressure along several isotherms. Curves representing the lowest five isotherms are calculated from the fit to Eq. (1). The predicted 1000K isotherm is derived from the straight, dashed line in Fig. 3.

FIG. 2. Measured viscosities at lower pressures are plotted up to 1.5 GPa as fractional deviations from the fit to Eq. 1. Error bars are estimates of 1σ values. Data from van der Gulik et al. (vdG, [2, 3]) are also shown. In order to maintain the clarity of the plot, data from Golubev [4] (taken up to 0.08 GPa) were not included; it can be seen below in Fig.4 that these data tend to lie at lower values than reported in [2, 3] for the same temperatures.

FIG. 3. Reduced viscosity is plotted against reduced residual entropy (Eqs. 2). The solid curve represents values (as calculated from [1]) along the line of vapor-liquid equilibrium [12] from (1K below) the critical point to the triple point (solid triangle). Data from van der Gulik et al. (vdG, [2, 3]) and from Golubev (Gol, [4]) are included. The scale at the top pertains to a 298K isotherm and gives the ratio of fluid density to that at the critical point. Densities range from that of the 1 bar gas (s=0) to a factor of 4.9 times the critical value. The straight, dashed line drawn through the data is used to calculate the 1000K isotherm in Fig. 1 and the deviations in Fig. 4.

FIG. 4. Measured viscosities are plotted as fractional deviations from the straight, dashed line in Fig. 3. Data from van der Gulik et al. (vdG, [2, 3]) and from Golubev (Gol, [4]) are included. The solid curve represents values (as calculated from [1]) along the line of vapor-liquid equilibrium [12], from (1K below) the critical point to the triple point.

FIG. 5. Reduced viscosity (Eqs. 2) is plotted against the quantity $(\rho/\rho_{crit})^4/(T/T_{crit})$, here normalized to the value at the critical point. Symbols are the same as in previous figures. The inset contains values of Γ (computed from [12, 16]) plotted against the melting temperature.

Fig. 1
Abramson
PRE

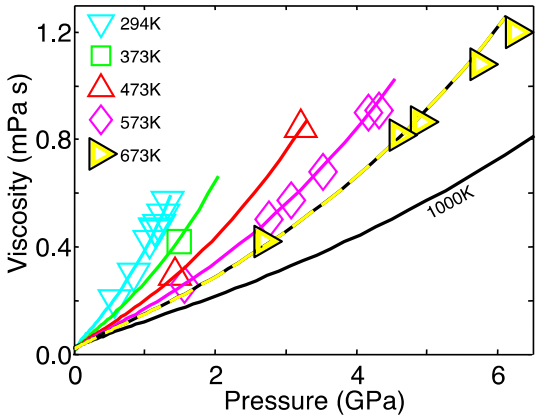

Fig. 2
Abramson
PRE

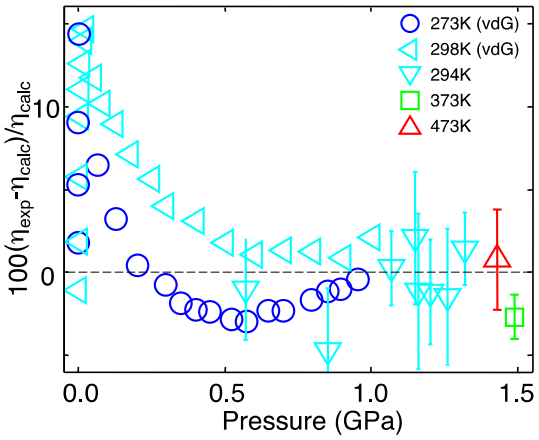

Fig. 3
Abramson
PRE

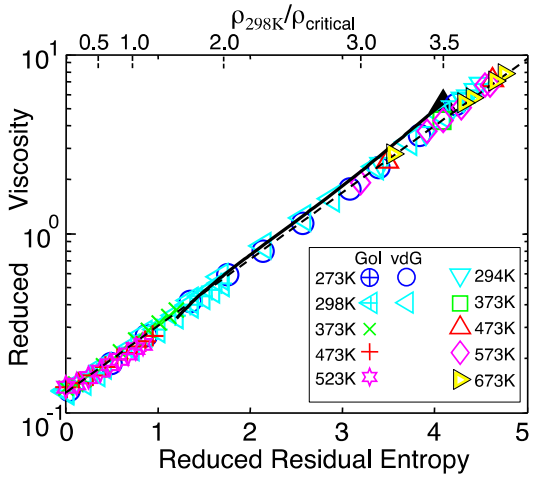

Fig. 4
Abramson
PRE

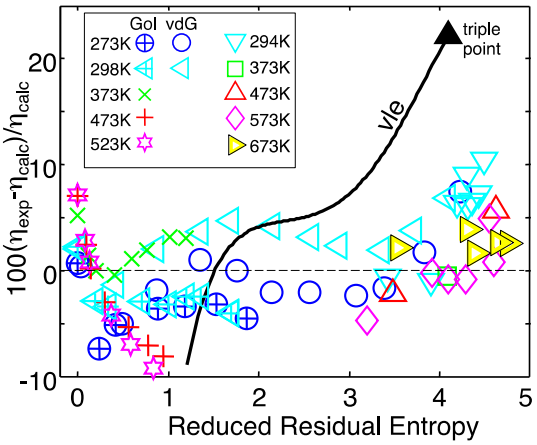

Fig. 5
Abramson
PRE

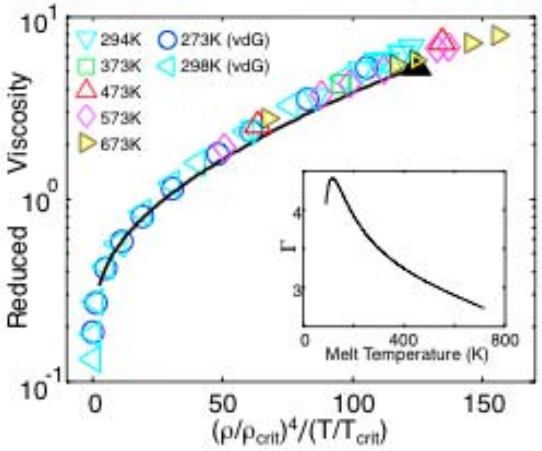

TABLE I. Measured pressures, temperatures, viscosities and nominal fractional uncertainties (1σ) of viscosities, with densities and reduced residual entropies from [12].

P(GPa)	T(K)	η(mPa s)	δ(%)	ρ(g cm^{-3})	. □
0.57	295.0	0.202	3	0.5089	3.42
0.85	294.3	0.303	4	0.5520	3.90
1.07	294.5	0.422	2	0.5781	4.20
1.15	294.7	0.472	4	0.5866	4.29
1.16	294.5	0.463	5	0.5876	4.31
1.20	294.8	0.484	3	0.5916	4.35
1.26	293.2	0.522	4	0.5979	4.44
1.32	294.5	0.568	2	0.6032	4.49
1.49	372.7	0.419	1	0.6016	4.08
1.43	473.7	0.294	3	0.5771	3.49
3.22	475.8	0.844	1	0.6965	4.62
1.56	576.3	0.257	3	0.5721	3.20
2.76	578.0	0.502	3	0.6578	3.92
3.08	574.5	0.574	2	0.6759	4.09
3.52	575.6	0.678	2	0.6979	4.28
4.17	575.2	0.901	3	0.7272	4.54
4.32	574.6	0.909	4	0.7335	4.60
2.69	676.8	0.419	2	0.6411	3.55
4.61	674.5	0.817	2	0.7340	4.31
4.90	674.8	0.864	4	0.7453	4.40
5.75	676.8	1.082	4	0.7757	4.65
6.26	684.7	1.199	5	0.7918	4.76